CD14 and NFAT mediate lipopolysaccharide-induced skin edema formation in mice

Ivan Zanoni, Renato Ostuni, Simona Barresi, Marco Di Gioia, Achille Broggi, Barbara Costa, Roberta Marzi, and Francesca Granucci

Department of Biotechnology and Biosciences, University of Milano-Bicocca, Milan, Italy.

Inflammation is a multistep process triggered when innate immune cells — for example, DCs — sense a pathogen or injured cell or tissue. Edema formation is one of the first steps in the inflammatory response; it is fundamental for the local accumulation of inflammatory mediators. Injection of LPS into the skin provides a model for studying the mechanisms of inflammation and edema formation. While it is known that innate immune recognition of LPS leads to activation of numerous transcriptional activators, including nuclear factor of activated T cells (NFAT) isoforms, the molecular pathways that lead to edema formation have not been determined. As PGE_2 regulates many proinflammatory processes, including swelling and pain, and it is induced by LPS, we hypothesized that PGE_2 mediates the local generation of edema following LPS exposure. Here, we show that tissue-resident DCs are the main source of PGE_2 and the main controllers of tissue edema formation in a mouse model of LPS-induced inflammation. LPS exposure induced expression of microsomal PGE synthase-1 (mPGES-1), a key enzyme in PGE_2 biosynthesis. mPGES-1 activation, PGE_2 production, and edema formation required CD14 (a component of the LPS receptor) and NFAT. Therefore, tissue edema formation induced by LPS is DC and CD14/NFAT dependent. Moreover, DCs can regulate free antigen arrival at the draining lymph nodes by controlling edema formation and interstitial fluid pressure in the presence of LPS. We therefore suggest that the CD14/NFAT/mPGES-1 pathway represents a possible target for antiinflammatory therapies.

Introduction

Inflammatory processes are initiated by innate immune system cells that perceive the presence of pathogens or microbial products through the expression of pattern recognition receptors (PRRs) (1). Following the encounter with their specific ligands, PRRs initiate a signal transduction pathway, leading to the activation of transcription factors that, in turn, regulate the expression of proinflammatory cytokines and costimulatory molecules that are important for the activation of innate and adaptive responses (2, 3). Among the PRRs, the receptor complex of the smooth form of LPS, a major constituent of the outer membrane of Gram-negative bacteria, is the best characterized. This particular receptor complex is composed of a series of proteins, including LPS-binding protein (LBP), MD2, CD14, and TLR4, required for LPS recognition, binding, and the initiation of the signaling cascade. We have recently demonstrated that CD14 is at the apex of all cellular responses to LPS (4) by controlling LPS recognition and TLR4 trafficking to the endosomal compartment with the consequent initiation of both the MyD88-dependent and TRIF-dependent pathways (5). At the end of the signaling cascade, different transcription factors, including NF-κB, activation protein 1 (AP-1), and IFN regulatory factors (IRFs), are activated (6).

Recently, the nuclear factor of activated T cells (NFAT) isoforms have also been included among the transcription factors activated through PRR signaling, particularly in conventional DCs. NFATs translocate to the nucleus following dectin 1 activation with curdlan and CD14 engagement by LPS (7, 8). Therefore, CD14 has signal transduction capabilities as well. While NF-κB and AP-1's roles in DCs following activation have been largely defined, for instance, regulation of inflammatory cytokine production, costimulatory molecule expression, antigen uptake, and processing and regulation of DC migration, most of the functions of NFAT remain to be elucidated. The only identified NFAT activities in activated DCs include regulation of IL-2 and IL-10 production and terminal differentiation and apoptotic death (7, 8).

In a scrutiny of data sets for the identification of genes regulated by the DC-specific CD14/NFAT signaling pathway triggered by LPS, we identified *Ptges1* as a potential transcriptional target (7). *Ptges1* codes a protein called microsomal PGE synthase-1 (mPGES-1). This protein, together with cytosolic PLA_2 ($cPLA_2$) and COX-2, coordinates a multistep biosynthetic process leading to the release of PGE_2 (9–11). In particular, following cell exposure to inflammatory stimuli, $cPLA_2$ translocates from the cytosol to the nuclear membrane, where it hydrolyzes membrane phospholipids to form arachidonic acid. Inflammatory stimuli also induce the expression of COX-2 and mPGES-1. COX-2 acts on arachidonic acid and converts it to PGG_2, which is in turn converted to PGH_2. Finally mPGES-1 converts PGH_2 to PGE_2. Therefore, all these 3 enzymes are required to generate PGE_2 (12), one of the most versatile prostanoids. PGE_2 is involved in the regulation of many physiological and pathophysiological responses, including local edema formation in inflammation through vasodilatation (13). We thus hypothesized that CD14-dependent NFAT activation in DCs was required for efficient PGE_2 production and, consequently, for the local generation of edema following LPS exposure.

Herein we report that this prediction was indeed correct and that local edema formation following LPS exposure is induced by tissue-resident DCs via PGE_2 production in a CD14-NFAT–dependent manner.

Results

Ptges-1 is a transcriptional target of NFAT in DCs upon LPS stimulation. We have recently observed that DC stimulation with LPS induces the activation of NFAT proteins (7). In particular, LPS

Authorship note: Ivan Zanoni and Renato Ostuni contributed equally to this work.
Conflict of interest: The authors have declared that no conflict of interest exists.
Citation for this article: *J Clin Invest.* 2012;122(5):1747–1757. doi:10.1172/JCI60688.

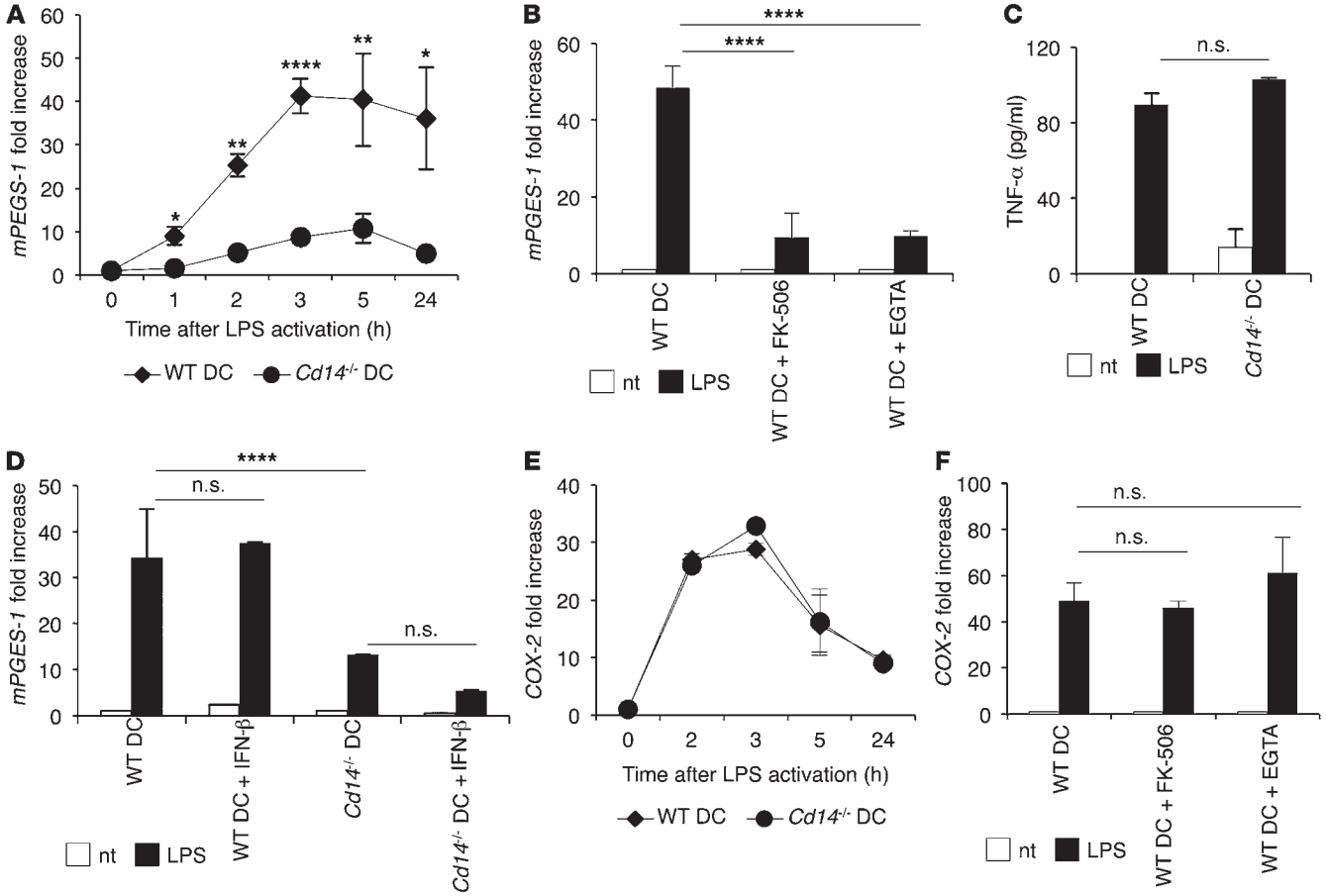

Figure 1

CD14-dependent NFAT activation induced by LPS in DCs regulates *mPGES-1* expression in vitro. (**A**) Real-time PCR analysis of *mPGES-1* mRNA induction kinetics in WT and CD14-deficient ex vivo DCs stimulated with LPS (1 μg/ml). (**B**) Upregulation of *mPGES-1* mRNA after 3 hours of LPS administration by ex vivo WT DCs pretreated with PBS, FK-506 (1 μM, 90 minutes), or EGTA (2 mM, 30 minutes). (**C**) Production of TNF-α by ex vivo WT and *Cd14*$^{-/-}$ DCs following LPS exposure evaluated by ELISA. (**D**) Upregulation of *mPGES-1* mRNA by ex vivo WT and *Cd14*$^{-/-}$ DCs treated or not with IFNβ (50 U/ml) 1 hour after LPS (total LPS treatment 3 hours). (**E**) Real-time PCR analysis of *COX-2* mRNA induction kinetics by WT and CD14-deficient ex vivo DCs stimulated with LPS (1 μg/ml). (**F**) Upregulation of *COX-2* mRNA after 3 hours of LPS administration by WT ex vivo DCs pretreated with PBS, FK-506 (1 μM, 90 minutes pretreatment), or EGTA (2 mM, 30 minutes pretreatment). Values represent means of at least 3 independent experiments performed in duplicate + SEM. **P* < 0.05; ***P* < 0.005; *****P* < 0.00005. nt, not treated.

induces the activation of Src family kinases and PLCγ2, the influx of extracellular Ca^{2+}, the consequent calcineurin activation, and finally, calcineurin-dependent nuclear NFAT translocation. The initiation of this pathway is independent of TLR4 engagement and depends exclusively on CD14 (Supplemental Figure 1; supplemental material available online with this article; doi:10.1172/JCI60688DS1).

To investigate the role of NFAT in DCs following LPS exposure, we previously performed a kinetic global gene expression analysis. Immature DCs were compared with activated DCs at different time points following LPS stimulation in conditions in which NFAT nuclear translocation was either allowed or not. *Ptges1* was selected among the specific NFAT targets (7).

Here, we validated this observation by quantitative RT-PCR (qRT-PCR) in mouse ex vivo and BM-derived DCs (BMDCs). We observed a strong induction of *mPGES-1* mRNA in WT DCs after LPS stimulation (Figure 1A and Supplemental Figure 2A), a response that was greatly impaired in *Cd14*$^{-/-}$ cells (Figure 1A and Supplemental Figure 2A). Blocking NFAT activation in ex vivo WT DCs by preincubating cells with the Ca^{2+} chelator EGTA or the calcineurin inhibitor FK-506 also resulted in reduced mPGES-1 expression (Figure 1B). The same results were obtained using BMDCs (Supplemental Figure 2B).

We excluded that a reduced activation of NF-κB accounted for the defective mPGES-1 upregulation in *Cd14*$^{-/-}$ DCs (14) by using doses of LPS (1 μg/ml) that allowed direct agonist detection by TLR4 without an absolute requirement for CD14, as evidenced by the ability of *Cd14*$^{-/-}$ DCs to normally secrete TNF-α (Figure 1C). Similarly, an impairment of CD14-dependent IRF3 activation (4, 15) could not explain our observations on mPGES-1 transcription. Coadministration of IFN-β (directly controlled by IRF3) did not restore mPGES-1 induction in LPS-treated *Cd14*$^{-/-}$ DCs (Figure 1D). Supporting the hypothesis of NFAT being the key factor, mPGES-1 induction by LPS correlated with the production of IL-2, a bona fide marker for NFAT activation in DCs (ref. 7 and Supplemental Figure 2C).

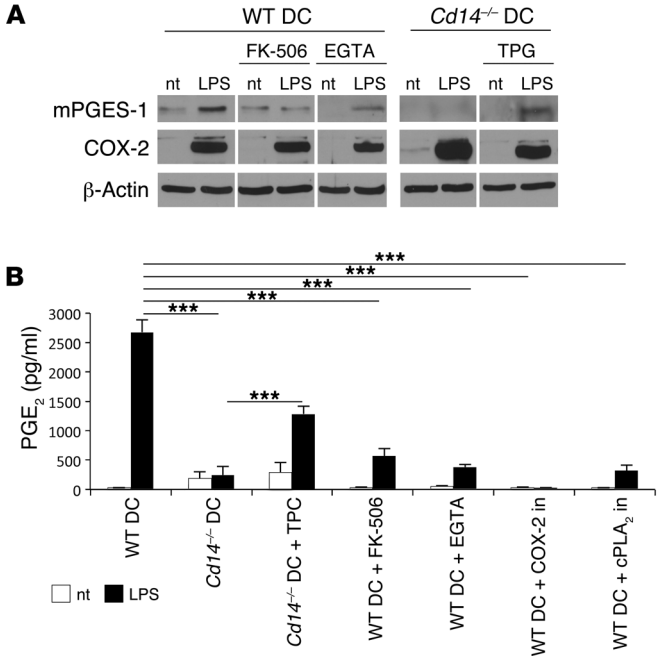

Figure 2

CD14-dependent NFAT activation induced by LPS in DCs regulates PGE_2 synthesis in vitro. (**A**) Western blot analysis of mPGES-1 and COX-2 induction in WT and CD14-deficient BMDCs 4 hours after LPS (1 μg/ml) and/or thapsigargin (TPG) (50 nM) treatment. Where indicated, the cells were pretreated with FK-506 or EGTA. The experiment was repeated 3 times with similar results. (**B**) PGE_2 production by ex vivo DCs 4 hours after LPS stimulation. WT and *Cd14*$^{-/-}$ DCs were treated with LPS or LPS plus thapsigargin (50 nM) or TPG alone; WT DCs were also treated with LPS and/or FK506, LPS and/or EGTA, LPS and/or COX-2 inhibitor (in) (1 μM, 30 minutes pretreatment), LPS and/or $cPLA_2$ inhibitor ($cPLA_2$ in, 1 μM, 30 minutes pretreatment). Values represent means of at least 3 independent experiments performed in duplicate + SEM. ***$P < 0.0005$.

The other key enzyme for PGE_2 production, COX-2, has been also reported to be regulated by NFAT in other experimental settings (16). Therefore, we determined whether CD14 influenced its expression. However, COX-2 induction by LPS in ex vivo DCs was not affected by CD14 deficiency (Figure 1E). Analogously, blocking Ca^{2+} fluxes or NFAT activation did not alter LPS-induced COX-2 expression by DCs (Figure 1F).

A Western blot analysis confirmed the expression data. As shown in Figure 2A, LPS induced mPGES-1 synthesis in WT, but not in *Cd14*$^{-/-}$, cells in a way dependent on Ca^{2+} fluxes and NFAT activation. Moreover, the deliberate induction of Ca^{2+} fluxes and NFAT activation by thapsigargin (ref. 7 and Supplemental Figure 2D) restored mPGES-1 upregulation in *Cd14*$^{-/-}$ DCs (Figure 2A). Conversely, LPS-induced COX-2 synthesis was not influenced by CD14 expression or NFAT activation (Figure 2A). Together, these results indicate that CD14-dependent NFAT activation controls mPGES-1 but not COX-2 expression.

PGE_2 production by DCs following LPS stimulation depends on CD14 and NFAT. We then measured the synthesis of PGE_2. Consistent with the mPGES-1 results, PGE_2 release in vitro was strongly impaired in *Cd14*$^{-/-}$ compared with WT DCs (Figure 2B and Supplemental Figure 3A). Moreover, blocking NFAT activation by blocking Ca^{2+} influx with EGTA or blocking calcineurin by means of FK-506 strongly affected LPS-induced PGE_2 production by WT DCs (Figure 2B and Supplemental Figure 3A). We were able to restore PGE_2 production in *Cd14*$^{-/-}$ DCs by coupling LPS stimulation with thapsigargin (Figure 2B). As control, we confirmed the necessary role of $cPLA_2$ and COX-2 for LPS-induced PGE_2 synthesis (Figure 2B and Supplemental Figure 3A). Moreover, the analysis of TNF-α production indicated that the tested conditions did not influence the pathway of NF-κB activation (Supplemental Figure 3B).

We have recently shown that different LPS species may elicit slightly different innate responses by initiating different signaling pathways (17). Therefore, we evaluated whether LPS from different sources were equally able to induce mPGES-1, COX-2, and PGE_2 production. As shown in Supplemental Figure 3, C–E, all of the tested LPS species induced mPGES-1 and COX-2 upregulation and PGE_2 production with a similar efficiency.

These data indicate that PGE_2 production by DCs following LPS stimulation depends on the Ca^{2+}/calcineurin pathway activation via the engagement of CD14. This pathway regulates mPGES-1, but not COX-2 expression.

Edema formation following LPS exposure depends on DCs. Following interaction with TLR agonists, DCs remain at the site of infection for the time necessary to take up the antigens (18, 19). During the time of persistence at the infected tissue, DCs actively participate in the sustainment of the inflammatory process (20, 21). Subsequently, DCs acquire the ability to migrate and reach the draining lymph nodes 2 to 3 days after infection (22, 23). Moreover, PGE_2 is well known to sustain the formation of edema at the inflammatory site during the innate phase of an immune response (13). Given the initial persistence of DCs at the site of inflammation and their ability to produce PGE_2, we investigated whether DCs could participate in edema formation. To this purpose, we used DOG mice, an animal model that expresses the diphtheria toxin receptor (DTR) under the control of the CD11c promoter. In these animals, an efficient conditional ablation of DCs can be induced by DT injections (24). By performing consecutive DT injections, we were able to conditionally ablate DCs in lymphoid and nonlymphoid organs and tissues including the skin (Figure 3A and Supplemental Figure 4, A–D). Importantly, such a treatment did not cause any significant alteration in either macrophage or granulocyte populations in the footpad (Figure 3A and Supplemental Figure 4, C and D). The quantitative analysis of cell population distribution in the selected peripheral tissue was performed by qRT-PCR of cell-specific mRNAs, as previously described (25), and by flow cytometry.

We compared paw edema formation after a single injection of LPS into the footpads of CD11c.DOG mice that were previously administered DT (CD11c.DOG-DT) or PBS (CD11c.DOG-NT).

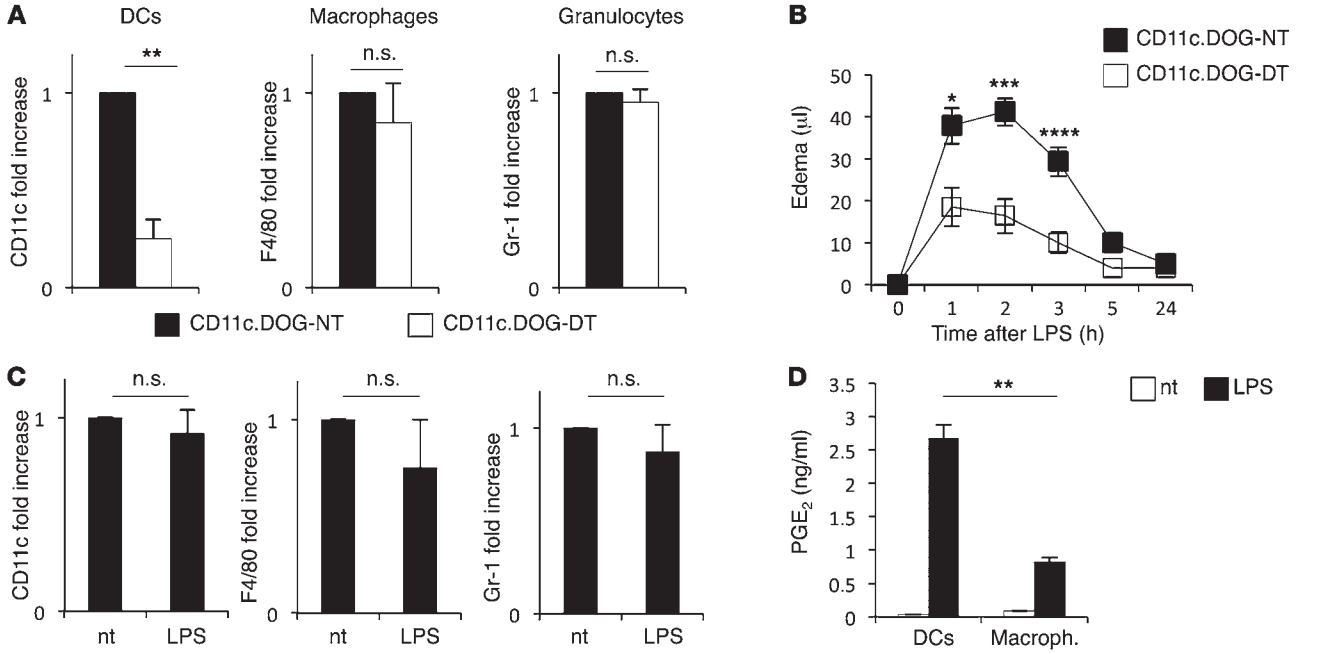

Figure 3

DCs regulate LPS-induced tissue edema formation. (**A**) Real-time PCR analysis of *CD11c*, *F4/80*, and *Gr-1* mRNA in the footpad of CD11c.DOG mice before (CD11c.DOG-NT) or after 2 rounds of DT (16 ng/g) treatment (CD11c.DOG-DT). Values represent at least 3 independent experiments with 3 mice per group + SEM. (**B**) Inflammatory swelling in the footpad of CD11c.DOG-NT and CD11c.DOG-DT mice measured at the indicated time points after s.c. injection of LPS (20 μg/footpad). Values represent means of at least 3 independent experiments with at least 3 mice per group + SEM. (**C**) Real-time PCR analysis of *CD11c*, *F4/80*, and *Gr-1* mRNA in the footpad of CD11c.DOG mice before and after 2 hours of s.c. LPS injection (20 μg/footpad). Values represent means of at least 3 independent experiments with 2 mice per group + SEM. (**D**) PGE_2 production in vitro by ex vivo DCs and macrophages (macroph.) ($F4/80^+$) after LPS stimulation. $^*P < 0.05$; $^{**}P < 0.005$; $^{***}P < 0.0005$; $^{****}P < 0.00005$.

Notably, DC depletion had a strong impact on tissue edema formation (Figure 3B), and the effect was also apparent with different LPS doses (Supplemental Figure 4E). This indicated that DCs play a major role in the generation of edema. Inflammatory swelling was mainly induced by tissue-resident DCs, since no local recruitment of DCs, macrophages, or granulocytes was observed early after LPS administration (Figure 3C and Supplemental Figure 5).

The transitoriness of edema formation correlated with the kinetics of COX-2 expression by DCs (Figure 1E and Figure 3B), suggesting that edema shutoff was dictated by COX-2 and not by mPGES-1.

The predominant role of DCs in tissue edema formation is also supported by the observation that LPS-stimulated ex vivo DCs secrete much higher levels of PGE_2 compared with ex vivo macrophages (Figure 3D). Nevertheless, a minor role for macrophages in vivo cannot be completely excluded.

Edema formation following LPS exposure is controlled by DCs and the CD14/NFAT pathway. DCs produce large amounts of PGE_2 after LPS exposure in vitro thanks to NFAT-regulated mPGES-1 expression. Moreover, tissue-resident DCs play a major role in edema formation in vivo at the inflammatory site generated by LPS injection. Therefore, we hypothesized that tissue-resident DCs could promote edema formation via the activation of the CD14/NFAT pathway and the consequent mPGES-1–mediated efficient PGE_2 production following LPS exposure.

We thus predicted that alterations in the PGE_2 biosynthetic pathway of DCs should recapitulate the LPS-unresponsive phenotype in terms of tissue swelling of DC-depleted mice. To this purpose, we compared LPS-induced paw edema in conditions that allow or do not allow NFAT activation in DCs. In particular, we analyzed WT, *Cd14*$^{-/-}$, and FK-506–treated mice for the development of paw edema after LPS administration. As shown in Figure 4, A and B, and Supplemental Figure 4F, significant swells developed in WT but not in *Cd14*$^{-/-}$ and FK-506–treated mice. The phenotype could be restored by cotreating *Cd14*$^{-/-}$ mice with LPS and thapsigargin, indicating a role for NFAT activation in this in vivo model of PGE_2-dependent inflammation (Figure 4C). Thapsigargin alone did not trigger a detectable inflammatory response in the paw (Supplemental Figure 6A). As a control, PGE_2 administration also induced edema formation in *Cd14*$^{-/-}$ animals (Figure 4C), and COX-2 inhibition affected edema formation in LPS-treated WT mice (Figure 4D).

To further substantiate the role of DC-derived PGE_2 in edema formation following LPS exposure, we conducted an in vivo analysis of *mPGES-1* and *COX-2* mRNA expression in the footpads of WT, *Cd14*$^{-/-}$, FK-506–treated, and DC-depleted mice. A global 3-fold transcriptional induction of mPGES-1 upon LPS treatment was observed in WT mice (Figure 5A), while it was completely lost in *Cd14*$^{-/-}$ and FK-506–treated mice (Figure 5, A and C). In contrast, COX-2 expression was not affected by the inhibition of the CD14/NFAT pathway (Figure 5, B and D).

We also measured *TNF*-α mRNA in the whole tissue under the same conditions as in controls. We observed a similar upregulation in WT, *Cd14*$^{-/-}$, and FK-506–treated mice (Supplemental Figure 6B), indicating that there was not a defect in LPS sensing.

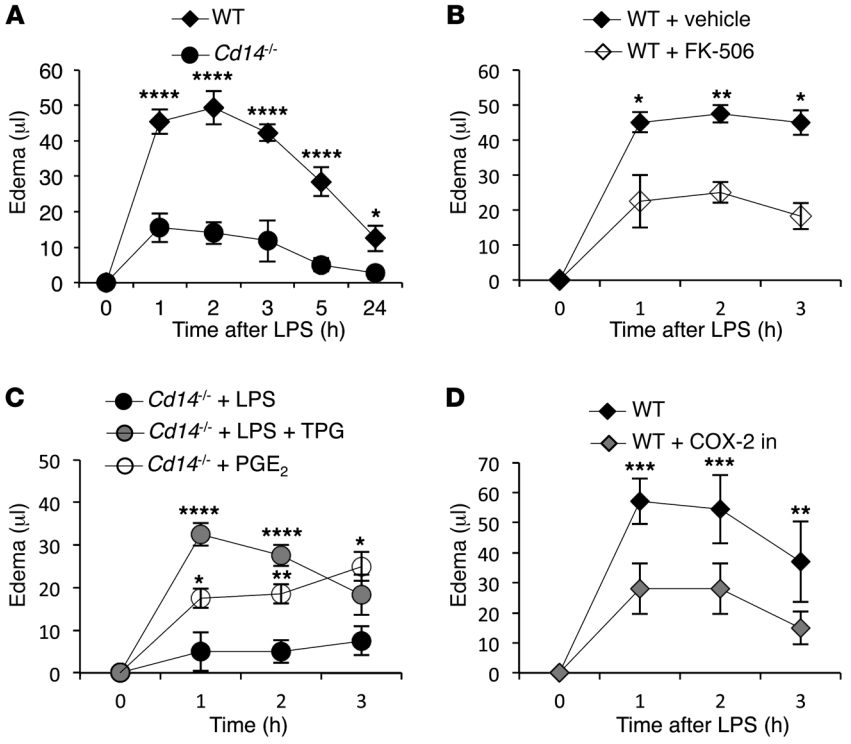

Figure 4
DCs regulate LPS-induced tissue edema formation through CD14-dependent and NFAT-dependent mPGES-1 expression. (**A**) Inflammatory swelling in the footpads of WT and *Cd14*$^{-/-}$ mice at the indicated time points after s.c. injection of LPS (20 μg/footpad). (**B**) Inflammatory swelling in the footpads of WT mice treated with LPS and pretreated or not with FK-506. (**C**) Inflammatory swelling in the footpads of CD14-deficient mice induced by LPS, LPS plus thapsigargin, or PGE_2 alone (10 nM). (**D**) Inflammatory footpad swelling induced by LPS in mice pretreated or not with the COX-2 inhibitor. Data represent 2 independent experiments with 5 mice per group. Means and SEM are shown. *$P < 0.05$; **$P < 0.005$; ***$P < 0.0005$; ****$P < 0.00005$.

Interestingly, depletion of DCs not only affected *mPGES-1* mRNA upregulation (Figure 5E), but also the local induction of *COX-2* and *TNF*-α mRNAs (Figure 5F and Supplemental Figure 6B). This observation and the capacity of DCs to regulate edema generation strongly reinforce the idea that DCs are crucial innate immune players that directly regulate the onset of inflammation.

Finally, we measured the amounts of PGE_2 secreted in vivo in the footpads in response to LPS. In complete agreement with the data on mPGES-1 expression, PGE_2 production was strongly affected in *Cd14*$^{-/-}$, NFAT-inhibited, and DC-depleted mice (Figure 5G).

Together, these data indicate that the reduction in paw edema observed in mice in which DCs were impeded in their CD14/NFAT signaling pathway was due to defective mPGES-1 upregulation.

DC-mediated edema formation controls free antigen arrival at the draining lymph nodes. Exogenous antigens present in the inflamed skin or administered s.c. are delivered at the lymph nodes in 2 successive waves. In the first wave, antigens freely diffuse through lymphatic vessels, and in the late wave, they are transported by DCs (26, 27), including $CD14^+$ dermal DCs (28). It is thought that one of the consequences of edema formation is the increase in the efficiency of free antigen arrival at the draining lymph nodes, since the rise of the interstitial pressure would force some of the fluid into lymphatic capillaries. To determine whether this is indeed the case, local edema was artificially generated by injecting increasing amounts of PBS into the footpad. FITC-labeled microbeads were also administered. As shown in Figure 6, the efficiency of bead arrival to the draining lymph node increased with a gain in edema volume. Interestingly, a minimum threshold of edema size was required to see the effect of antigen delivery. Therefore, we predicted that the ability of DCs to control tissue swelling in the presence of LPS could have as a consequence the control of the first wave of antigen arrival to the lymph nodes. To investigate this question, we evaluated FITC-dextran delivery and FITC-coupled bead delivery.

We first performed s.c. injections of dextran in conditions either permitting or not permitting edema formation, and we analyzed the efficiency of dextran uptake by $CD11b^+$ phagocytes in the draining lymph nodes 2 hours after treatment. As a control, we verified that LPS treatment and NFAT inhibition did not affect DC and macrophage absolute numbers in the draining lymph nodes during the first 3 hours after LPS injection (Supplemental Figure 7, A and B). We compared mice treated with LPS and dextran with mice treated exclusively with dextran, and mice treated with dextran plus LPS plus FK-506 (to inhibit the NFAT pathway) with mice treated with dextran plus FK-506. As shown in Figure 7A, a clear increase in the efficiency of dextran lymph node arrival was measurable in the presence of LPS. This increase was completely abrogated by FK-506 treatment. Moreover, the LPS-mediated increase in dextran lymph node arrival was also nullified when the mice were deprived of DCs (Figure 7A) and therefore were deprived of the capacity to form paw edema in response to LPS (Figure 3B).

To exclude that the treatment with FK-506 could have influenced the intrinsic efficiency of phagocyte uptake, we repeated the experiment by directly administering PGE_2 to deliberately induce edema formation (Figure 7B). When PGE_2 was added in combination with LPS and FK-506, a clear increase in phagocyte dextran uptake was observed compared with that in the untreated (dextran only) mice. The increase in uptake was also observable in the animals treated with PGE_2 and FK-506 compared with the untreated animals (dextran only), indicating that FK-506

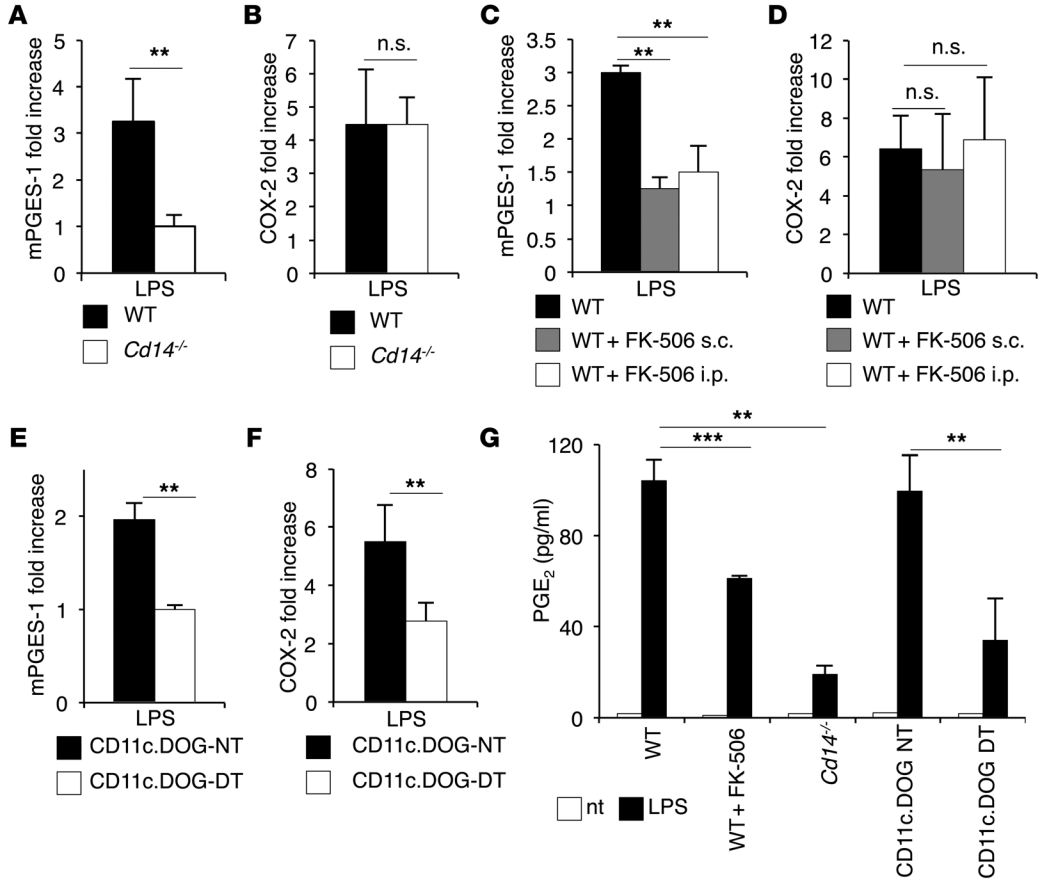

Figure 5

CD14-dependent NFAT activation induced by LPS in DCs regulates mPGES-1 expression and PGE_2 synthesis in vivo. Real-time PCR analysis of (**A**, **C**, and **E**) *mPGES-1* and (**B**, **D**, and **F**) *COX-2* mRNA induction 2 hours after LPS injection in the footpads of WT and *Cd14*$^{-/-}$ mice. (**C** and **D**) WT mice were pretreated with FK-506 s.c. or i.p. (**E** and **F**) CD11c.DOG mice treated or not with DT. Values represent at least 2 independent experiments ($n = 5$) + SEM. (**G**) PGE_2 production in vivo induced by LPS in WT, CD14-deficient, and CD11c.DOG mice treated or not with DT. Measurement was performed 3 hours after LPS administration. Where indicated, WT mice were pretreated for 18 hours with FK-506 (s.c.). Data represent 3 independent experiments with 3 animals per group + SEM. $^{**}P < 0.005$; $^{***}P < 0.0005$.

treatment does not influence antigen uptake capacity of $CD11b^+$ cells, but only the capacity of antigen arrival at the lymph nodes by inhibiting edema formation. To further prove that the inhibition of the Ca^{2+}/NFAT pathway did not affect the antigen uptake capacity of phagocytic cells, we measured the increase of dextran uptake of DCs (Figure 7C) and macrophages (data not shown) after LPS stimulation in the presence of FK-506 or EGTA. The uptake efficiency was not reduced by these treatments (Figure 7C), confirming our hypothesis.

The described approach did not allow us to directly investigate the involvement of CD14 in controlling the amount of antigen that arrives at the lymph nodes as a consequence of edema formation. We have, indeed, recently shown that CD14 influences the efficiency of antigen uptake (4). Therefore, we used the second method. FITC-labeled microbeads were injected in the footpads of WT and *Cd14*$^{-/-}$ animals in the presence or absence of LPS and the numbers of microbeads reaching the draining lymph node enumerated 3 hour later, a time point compatible with free antigen arrival and not with DC migration (22). While in WT animals, the efficiency of bead trafficking was strongly increased by LPS (Figure 8A), in *Cd14*$^{-/-}$ mice, LPS treatment did not influenced the capacity of microbead arrival at the lymph nodes (Figure 8B). A clear increase in the numbers of microbeads in the lymph nodes was instead observed in *Cd14*$^{-/-}$ mice treated with PGE_2 to deliberately induce edema formation (Figure 8B). As previously observed, the treatment of WT animals with FK-506 nullified the LPS-mediated increase of free antigen arrival at the draining lymph nodes (Figure 7A).

To investigate whether the increase in the efficiency of antigen trafficking to draining lymph nodes induced by edema was sufficient to influence the efficiency of adaptive responses, OVA-coated beads were recovered from lymph nodes of WT mice treated with LPS in the presence or absence of FK-506 and from lymph nodes of *Cd14*$^{-/-}$ mice treated with LPS in the presence or absence of PGE_2. The recovered beads were then used to measure the proliferation capacity of OVA-specific OT-II cells in vitro. As shown in Figure 8, C and D, OT-II cells proliferated more efficiently when challenged with the amount of antigen recovered in all the conditions allowing edema formation. Therefore, the inhibition of CD14-dependent edema formation clearly has an impact on antigen arrival to the draining lymph nodes.

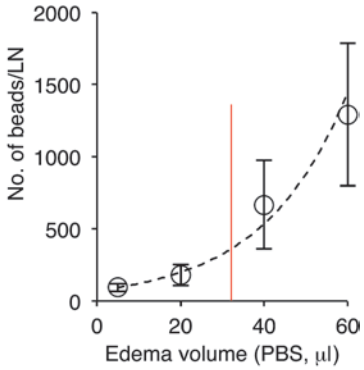

Figure 6
The efficiency of free antigen arrival at the draining lymph nodes increases with the increase of edema volume. Absolute numbers of FITC-labeled microbeads reaching the draining lymph nodes in WT mice injected in the footpad with the indicated PBS volumes. Dotted line represents an interpolated exponential curve with $R^2 = 0.98$. Red line represents the putative threshold of edema volume required to observe an effect on antigen delivery. Data are expressed and plotted as mean ± SEM values.

Discussion

DCs are involved in the regulation of many different aspects of innate and adaptive immunity. Following activation with PRR agonists, they sequentially acquire the ability to produce soluble and cell surface molecules critical for the initiation and control of innate and then adaptive immune responses. The production of these factors is regulated by the activation of NF-κB and AP1 downstream PRRs. Nevertheless, we have recently described that following smooth LPS exposure different NFAT isoforms are also activated (7). The initiation of the pathway that leads to nuclear NFAT translocation is totally dependent on CD14 that, through the involvement of src family kinases and PLC2, leads to Ca^{2+} mobilization and calcineurin activation. Nuclear NFAT translocation is required for IL-2 production and apoptotic death of terminally differentiated DCs. In the present work, we show that mPGES-1 and its direct product PGE_2 are also efficiently produced by DCs upon activation of the CD14-dependent Ca^{2+}/calcineurin and NFAT pathway.

Although COX-2 expression has been reported to be NFAT dependent in some experimental settings, we did not find any NFAT signaling pathway dependence of DC-produced COX-2 in response to LPS. A possible explanation of this discrepancy can be found in the fact that in the nucleus, the NFATc1-c4 isoforms need to interact with partner proteins, generically termed NFATn, to produce active NFAT transcription complexes. Usually, NFATc and NFATn are activated via distinct signaling pathways. NFATn in innate immunity is mostly unknown. It is possible that the NFATn factors required for the generation of the active NFATc-NFATn heterodimers capable of binding COX-2 promoter are not activated in DCs, while they are activated in other cell types.

The production of PGE_2 by DCs is particularly relevant in adaptive immune responses, since this prostanoid has been shown to regulate diverse DC functions, including DC migration and polarization of T cell responses (29, 30), by acting on different receptors in an autocrine or paracrine way (31). For instance, DC-derived PGE_2 facilitates Th1 differentiation through the EP1 receptor expressed by naive T cells (31), while PGE_2-mediated activation of the EP2 and EP4 receptors promotes Th2 differentiation (32, 33). Given the importance of PGE_2 for the regulation of DC functions, this prostanoid is one of the components of the nonmicrobial stimuli cocktail used to activate DCs for in vivo therapies.

During the innate phase of an immune response, it is well known that PGE_2 sustains the formation of edema at the inflammatory site (34). Consistent with this, we have observed that LPS-activated, tissue-resident DCs contribute to the formation of edema via the activation of the NFAT signaling pathway. *Cd14*$^{-/-}$ mice are almost totally incapable of generating edema at the LPS injection site, and this function can be restored by deliberately inducing Ca^{2+} mobilization and NFAT activation. The inefficient edema formation in the absence of CD14 cannot be attributed to a reduced responsiveness of the mutant mice to the dose of LPS used in this study. *Cd14*$^{-/-}$ mice could, indeed, produce TNF as efficiently as WT mice. Though the crucial CD14 role in the recognition of low LPS doses has been established, CD14 has been shown to be largely dispensable for the response to high concentrations of LPS, which occurs almost normally in *Cd14*$^{-/-}$ macrophages and DCs (4, 7, 35). This observation suggests that a high dose of LPS can also be sensed in a CD14-independent way, possibly through a direct LPS recognition by TLR4:MD-2 (36) or the participation of different LBPs (37).

The absence of CD14 and the knockdown of DCs affect the formation of edema in a very similar way, suggesting that CD14 exerts its contribution to LPS-induced edema almost exclusively through DCs. We thus assume that activation of the NFAT pathway for edema formation must occur predominately/exclusively in DCs. This observation is in agreement with our previous data showing that the CD14/NFAT pathway is not active in macrophages (7).

Neutrophils do not play a major role in LPS-induced edema formation at the cutaneous level. These results are consistent with the faster kinetics of tissue edema formation (1–2 hours) as compared with immune cell, including neutrophil, recruitment.

On first analysis, the participation of DCs in edema formation could seem surprising, since DCs leave the tissue after activation. Nevertheless, DCs do not acquire the ability to migrate immediately after LPS encounters; conversely, they persist in the peripheral tissue to maximize antigen uptake (18). As a matter of fact, antigen uptake and migration have been proposed to be two mutually exclusive DC activities (19). Early in the course of inflammation, in addition to performing antigen uptake, DCs contribute to the generation of edema via PGE_2 production.

It is important to note that PGE_2 is also involved in the control of DC migratory activity, in addition to the regulation of edema formation (38, 39). These 2 PGE_2 functions are not contradictory. DC-derived PGE_2 controls DC migration in an autocrine and indirect way by inducing the efficient production of MMP-9 following LPS encounter. PGE_2-induced MMP-9 occurs several hours after DC activation (40). MMP-9, in turn, regulates DC migration by contributing to the degradation of the basal membrane (40). Thus, the capacity to control edema formation and migratory activity are

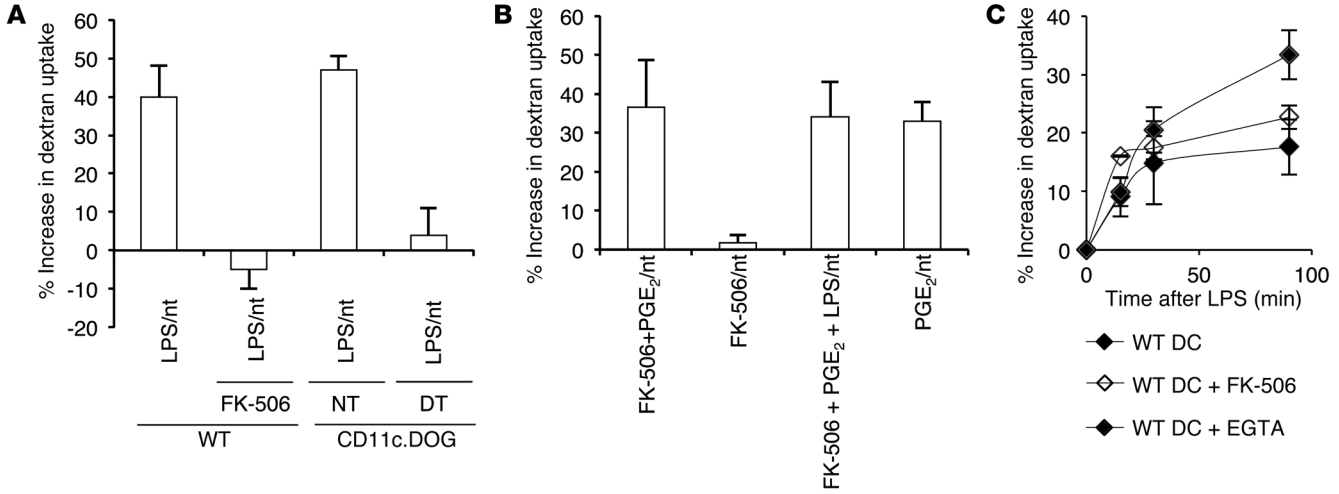

Figure 7

Edema induced by LPS increases the efficiency of dextran arrival at the draining lymph nodes. (**A**) Percentage of LPS-induced increase of dextran uptake by CD11b$^+$ cells in the lymph nodes draining the injection site. Measures were performed in WT and CD11c.DOG mice. Where indicated, WT mice were pretreated for 18 hours with FK-506. CD11c.DOG mice were treated or not with DT. Data have been calculated as percentage of uptake increase at the indicated conditions, considering as 100% the dextran uptake in the absence of any other stimulus. LPS/nt, percentage of increase of dextran uptake in mice treated with LPS plus dextran compared with dextran-treated mice. (**B**) Percentage of PGE_2-induced increase of dextran uptake by CD11b$^+$ cells in the lymph nodes draining the site of injection at the indicated conditions. FK-506 plus PGE_2/nt, percentage of increase of dextran uptake in mice pretreated with FK-506 and treated with PGE_2 plus dextran compared with dextran-treated mice; FK-506/nt, percentage of increase of dextran uptake in mice pretreated with FK-506 and treated with dextran compared with dextran-treated mice; FK-506 plus PGE_2 plus LPS/nt, percentage of increase of dextran uptake in mice pretreated with FK-506 and treated with PGE_2 plus LPS plus dextran compared with dextran-treated mice; PGE_2/nt, percentage of increase of dextran uptake in mice treated with PGE_2 plus dextran compared with dextran-treated mice. Experiments were repeated twice with 3 mice per group each time. Means ± SEM are shown. (**C**) Increase in the efficiency of dextran uptake (1 mg/ml) by BMDCs treated in vitro with LPS for the times indicated. Where specified, cells were pretreated with FK-506 and EGTA.

2 DC functions regulated by the same molecule, but segregated in time. Upon challenge with LPS, PGE_2 derived from DCs initially controls edema formation; later on, it regulates DC migration by inducing the synthesis of MMP-9.

Edema formation is one of the first steps in the generation of the inflammatory process, and it is a fundamental process for the local accumulation of inflammatory mediators. We show here that local swelling is also relevant for free antigen transport to the draining lymph nodes. Antigens present in the inflamed tissues are delivered to the lymph nodes in 2 successive waves. In the first wave, antigens freely diffuse through lymphatic vessels and in the late wave are transported by DCs (26, 27). The increase of the interstitial pressure due to edema forces some of the fluid into lymphatic capillaries and favors free antigen entry into the afferent lymphatics and free antigen arrival to the draining lymph nodes. Thus, we propose that tissue-resident DCs control not only the second wave of antigen arrival, but also the efficiency of the first wave by controlling edema formation. Both waves are then important for efficient activation of adaptive T cell responses (26, 41). Early antigen presentation by lymphoid-resident DCs is required to initiate activation and trapping of antigen-specific T cells in the draining lymph nodes, but is not sufficient for inducing clonal T cell expansion. Efficient proliferation is instead induced by migratory DCs arriving later to the draining lymph nodes (41).

DCs are extremely versatile cells, and our data suggest that they are one of the key players in a model of LPS-induced inflammation in vivo. They exert this primary role through their peculiar ability to respond to LPS through the initiation of the CD14/NFAT pathway, leading to the formation of edema. CD14 comes out as one of the master regulators of DC biology, as already shown in previous studies (4, 7, 42).

We propose the concept that DCs control skin edema formation following LPS exposure via the activation of 2 independent pathways: (a) the CD14/NFAT pathway, which regulates mPGES-1 production, and (b) the canonical NF-κB pathway, which controls COX-2 expression.

Most of the COX-2 inhibitors also inhibit COX-1 and, when used as antiinflammatory drugs, have severe toxic secondary effects, given the importance of COX-1 in tissue homeostasis. Our findings suggest that targeting the CD14/NFAT/mPGES-1 pathway in DCs may constitute a strategy to overcome such problems by selectively blocking the biosynthesis of PGE_2 in specific inflammatory settings.

Methods

Cells. BMDCs were derived from BM progenitors of WT or mutant mice as previously described (7). Ex vivo DCs were purified as previously described (43). Ex vivo macrophages were purified from spleen. Splenic unicellular suspensions were stained with biotinylated anti-F4/80 antibodies and positively selected using MACS beads according to the manufacturer's instructions (Miltenyi Biotec).

Mice. C57BL/6 mice and OT-II transgenic mice were purchased from Harlan. *Cd14*$^{-/-}$ mice were purchased from CNRS, Campus d'Orléans. N. Garbi (Institute of Molecular Medicine and Experimental Immunology, Bonn, Germany) provided CD11c.DOG mice expressing DTR under the control of the long CD11c promoter. In these mice, a specific DC ablation

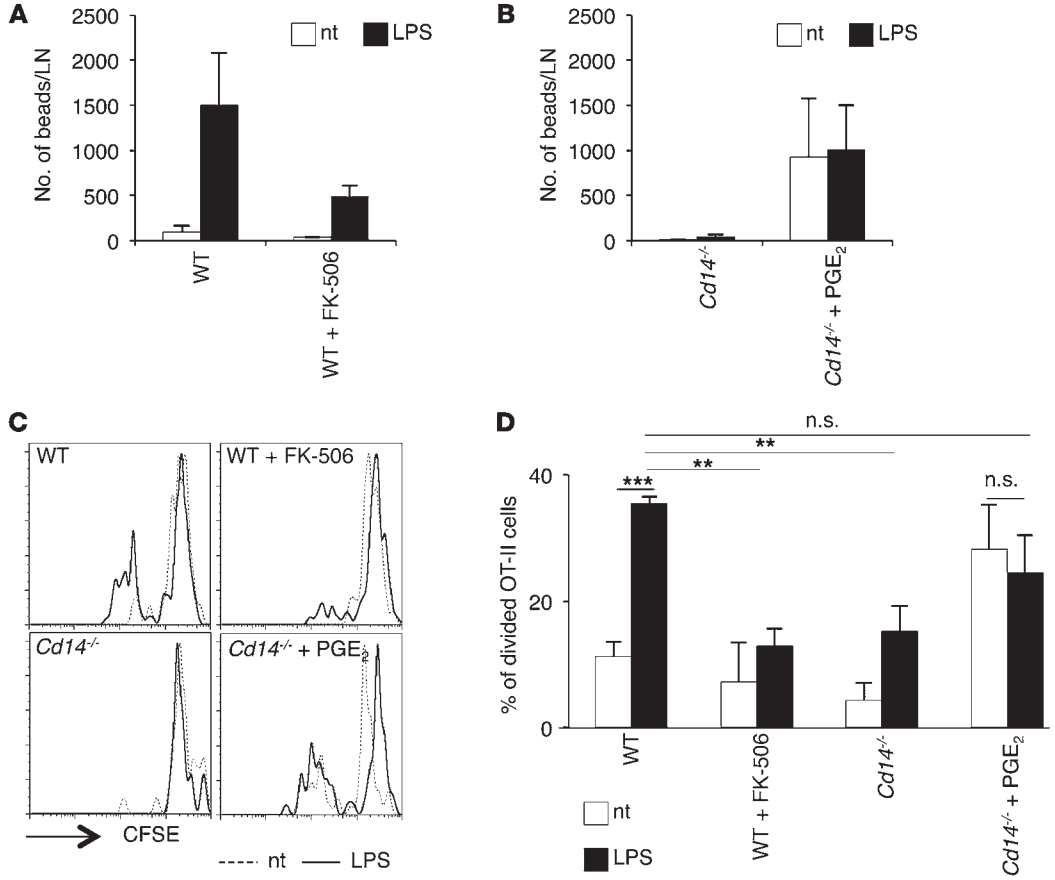

Figure 8

Edema induced by LPS increases the efficiency of bead arrival at the draining lymph nodes. (**A**) Absolute numbers of FITC-labeled microbeads reaching the draining lymph nodes in WT mice treated or not with LPS (4 hours after treatment). Where indicated, mice were pretreated s.c. with FK-506 for 18 hours. (**B**) Absolute numbers of FITC-labeled microbeads reaching the draining lymph nodes in CD14-deficient mice treated or not with LPS. Where indicated, mice were cotreated with PGE_2. (**A** and **B**) Data represent mean and SEM of at least 10 animals per group. (**C** and **D**) OT-II cell proliferation in response to the amount of antigen recovered from the lymph nodes of WT or CD14-deficient mice treated or not with LPS. Where indicated, the mice were cotreated with LPS and PGE_2 or pretreated s.c. with FK-506 for 18 hours. (**C**) FACS histograms. (**D**) Histogram quantification. Data represent mean and SEM of at least 6 animals per group. $^{**}P < 0.005$; $^{***}P < 0.0005$.

can be induced by diphtheria toxin injection (24). All animals were housed under pathogen-free conditions, and all experiments were carried out in accordance with relevant laws and institutional guidelines.

Antibodies and chemicals. Antibodies were purchased from BD Biosciences. TLR4-grade smooth LPS (*E. coli*, O55:B5; *E. coli*, O111:B4; *E. coli*, R515 [Re]; *E. coli*, lipid A; *Salmonella typhimurium*, S-form) were purchased from Enzo Life Sciences. CFSE was from Invitrogen. EGTA, PGE_2, FITC-dextran, FK-506, and thapsigargin were purchased from Sigma-Aldrich. Recombinant murine IFN-β and diphtheria toxin were purchased from R&D Systems. Antibody against murine mPGES-1 and COX-2, COX-2–specific inhibitor (NS-398), and $cPLA_2$ inhibitor (pyrrophenone) were purchased from Cayman Chemical. EndoGrade ovalbumin was purchased form Hyglos Gmbh. Fluoresbrite Carboxy YG 1-μm latex beads were from Polysciences. For adsorption of ovalbumin onto latex beads, microspheres were resuspended in ovalbumin (1 mg/ml) and incubated overnight at 4°C. Latex beads were then washed 15 times in large volumes of sterile endotoxin-free PBS.

In vivo treatment with FK-506. For in vivo treatment, FK-506 was resuspended in 40% w/v HCO-60/ethanol. Mice were injected s.c. (10 μg/footpad) or i.p. (40 μg/mouse) with FK-506 18 hours before stimuli injection.

DC depletion. Diphtheria toxin (16 ng/g) was daily administered to CD11c.DOG mice through an i.p. injection for 2 consecutive days. Control mice were given PBS. Effective DC depletion was assessed by FACS and qRT-PCR analysis.

Ex vivo PGE_2 extraction. Paw tissue was homogenized in 500 μl of PBS using a TissueLyser (QIAGEN) (full speed for 8 minutes). Samples were then centrifuged for 90 seconds at 5,000 *g*. The supernatant were collected into a new Falcon tube, and 2 ml of 100% EtOH was added and incubated 5 minutes at 4°C.

Samples were centrifuged for 10 minutes at 1,000 *g* and supernatants collected into a new Falcon tube. Then 8 ml PPS buffer (0.1 M, pH = 3) was added.

A Solid Phase Extraction (SPE) cartridge (C-18) was activated by rinsing with 5 ml 100% EtOH and then with 5 ml of water. Samples were passed through a column, which was then washed with 5 ml of water and 5 ml of exane. Samples were eluted by gravity with 5 ml ethyl acetate containing 1% methanol. The ethyl acetate was then evaporated and samples resuspended in an appropriate buffer for PGE_2 ELISA analysis.

ELISA assays. Concentrations of IL-2 and TNF-α in supernatants were assessed by ELISA kits purchased from R&D Systems. PGE_2 levels were assayed with a Monoclonal EIA Kit from Cayman Chemical.

Quantitative real-time PCR in vitro. Cells (2×10^6) were lysed with the TRIzol reagent (Applied Biosystems), and total mRNA was extracted with an RNeasy Mini Kit (QIAGEN) according to the manufacturer's instructions. A NanoDrop spectrophotometer (Thermo Scientific) was used to quantify mRNA and to assess its purity, and 600 ng mRNA was retrotranscribed to cDNA using a High-Capacity cDNA Reverse Transcription Kit (Applied Biosystems). Then 10 ng cDNA was amplified using the Power SYBR Green PCR Master Mix (Applied Biosystems) in a 7500 Fast Real-Time PCR System (Applied Biosystems), and data were analyzed using the built-in software.

Primer pairs used were as follows: 5′-ACGACATGGAGACAATCTATCCT-3′ and 5′-TGAGGACAACGAGGAAATGT-3′(mPGES-1); 5′-CCTGCTGCCCGACACCTTCAA-3′ and 5′-TCTTCCCCCAGCAACCCGGC-3′ (COX-2); and 5′-CGAAAGCATTTGCCAAGAAT-3′ and 5′-AGTCGGCATCGTTTATGGTC-3′ (18S). 18S mRNA was used as an internal reference for relative quantification studies.

Quantitative real-time PCR in vivo. Whole skin from treated or control mice was cut, briefly washed in cold PBS, and immersed in RNAlater solution (Ambion) at 4°C for 24 hours. Skin was then lysed in TRIzol and mechanically disrupted using a TissueLyser (QIAGEN) (30 shakes/s for 3 minutes). Subsequent mRNA processing was performed as described above.

Primer pairs used were as follows: 5′-TTTGTTTCTTGTCTTGGCTTCAA-3′ and 5′-TTAGTGGCTTTTATTTCCTTTGGT-3′(CD11c); 5′-CACCTTCATTTGCATCAACA-3′ and 5′-TCTGAAAAGTTGGCAAAGAGAA-3′(F4/80); and 5′-TGCTCTGGAGATAGAAGTTATTGTG-3′ and 5′-TTACCAGTGATCTCAGTATTGTCCA-3′ (Gr-1).

Primer pairs for mPGES-1, COX-2, and 18S are indicated above. Prevalidated QuantiTect primer pairs for TNF-α and HPRT1 (reference gene) were purchased from QIAGEN.

Isolation of skin cells. Cells were isolated as previously described (44). Briefly, skin was isolated and digested for 45 minutes in a cocktail containing collagenase XI, hyaluronidase, and DNase. Then 10% FBS was added to stop the reaction, and cells were stained to asses the percentage of different cell populations.

Tissue edema. Following anesthesia with pentobarbital (60 mg/kg), sex- and age-matched mice were injected s.c. with LPS (20 μg/20 μl), LPS plus thapsigargin (5 μM), and LPS plus PGE_2 or PGE_2 alone (10 μM) or PBS as a control in the footpad. In some cases, mice were pretreated with COX-2 inhibitor (30 minutes, 10 mg/kg), FK-506 (18 hours), or were depleted of DCs as previously described. The paw volume of the LPS-treated as well as the PBS-treated contralateral paw was then measured by a plethysmometer (Ugo Basile) at the indicated time points. At the 1-hour time point, most of the animals had recovered from the anesthesia, and at the 2-hour time point, all animals had recovered. The volume of the contralateral paw was subtracted from the volume of the injected paw to obtain edema volume.

Antigen delivery to the lymph node. Following anesthesia, sex- and age-matched mice were injected s.c. with the described combinations of LPS (15 μg), FITC-dextran (500 μg), or FITC–latex beads conjugated or not with ovalbumin (100.000 beads/footpad) and PGE_2 (10 μM) in the footpad (20 μl/footpad). In some cases, mice were pretreated with FK506 or were depleted of DCs as previously described. Two to four hours after injection, mice were sacrificed, draining lymph nodes collected, and bead numbers and dextran uptake by $CD11b^+$ cells measured by FACS analysis.

In vitro antigen presentation assay. Anti-ovalbumin $CD4^+$ T cells were purified by positive selection from spleen and lymph nodes of OT-II mice using anti-CD4–conjugated microbeads (Miltenyi Biotec) according to the manufacturer's instructions. Cells were then CFSE labeled according to the manufacturer's instructions.

Ovalbumin-coated latex beads were recovered from draining lymph nodes of mice. In particular, axillary and brachial lymph nodes were removed 3 hours after s.c. injection of the described stimuli. Lymph nodes were dissected in water and centrifuged at 5,000 *g* for 2 minutes to recover latex beads. The recovered beads were added to U-bottom 96-well plate of medium with 10,000 BMDCs, 50,000 OT-II $CD4^+$ CFSE-labeled T cells, and 10 ng/ml LPS (final volume 200 μl). After 120 hours, cell division was measured using FACScalibur.

Western blot. Cells were lysed with a buffer containing 50 mM Tris-HCl, pH 7.4, 150 mM NaCl, 10% glycerol, 1% NP-40 supplemented with protease, and phosphatase inhibitor cocktails (Roche). Cell debris were removed by centrifugation at 16,000 *g* for 15 minutes (4°C), and proteins were quantified using a BCA assay (Thermo Scientific). 10 μg cell lysate was run on a 10% polyacrylamide gel, and SDS-PAGE was performed following standard procedures. After protein transfer, nitrocellulose membranes (Thermo Scientific) were incubated with the indicated antibodies and developed using an ECL substrate reagent (Thermo Scientific).

Statistics. Means were compared by 2-tailed Student's *t* tests, unequal variance. Data are expressed and plotted as mean ± SEM values. Statistical significance was defined as $P < 0.05$. Sample sizes for each experimental condition are provided in the figures and the respective legends.

Study approval. The experimental protocols were approved by the Italian Ministry of Health (Rome, Italy) according to the Decreto legislativo 27 gennaio 1992, n. 116 "*Attuazione della Direttiva n. 86/609/CEE in materia di protezione degli animali utilizzati a fini sperimentali o ad altri fini scientifici*."

Acknowledgments

This work was supported by grants from the European Union FP7 Program (TOLERAGE: HEALTH-F4-2008-202156, ENCITE: HEALTH-F4-2008-201842), the Associazione Italiana per la Ricerca sul Cancro (AIRC), the Italian Ministry of Education and Research (PRIN 2009), the Fondazione Cariplo (grant 2010-0678), and Regione Lombardia (LIIN and ASTIL projects).

Received for publication November 25, 2011, and accepted in revised form February 15, 2012.

Address correspondence to: Francesca Granucci, Department of Biotechnology and Biosciences, University of Milano-Bicocca, Piazza della Scienza 2, 20126 Milan, Italy. Phone: 390264483553; Fax: 390264483553; E-mail: francesca.granucci@unimib.it.

1. Medzhitov R, Janeway CA Jr. How does the immune system distinguish self from nonself? *Semin Immunol*. 2000;12(3):185–188.
2. Banchereau J, Steinman RM. Dendritic cells and the control of immunity. *Nature*. 1998; 392(6673):245–252.
3. Medzhitov R, Preston-Hurlburt P, Janeway CA Jr. A human homologue of the Drosophila Toll protein signals activation of adaptive immunity. *Nature*. 1997;388(6640):394–397.
4. Zanoni I, et al. CD14 Controls the LPS-induced endocytosis of toll-like receptor 4. *Cell*. 2011; 147(4):868–880.
5. Foster SL, Medzhitov R. Gene-specific control of the TLR-induced inflammatory response. *Clin Immunol*. 2009;130(1):7–15.
6. Kaisho T, Akira S. Toll-like receptor function and signaling. *J Allergy Clin Immunol*. 2006;117(5):979–987.
7. Zanoni I, et al. CD14 regulates the dendritic cell life cycle after LPS exposure through NFAT activation. *Nature*. 2009;460(7252):264–268.
8. Goodridge HS, Simmons RM, Underhill DM. Dectin-1 stimulation by Candida albicans yeast or zymosan triggers NFAT activation in macrophages and dendritic cells. *J Immunol*. 2007;178(5):3107–3115.
9. Vane JR, Bakhle YS, Botting RM. Cyclooxygenases 1 and 2. *Annu Rev Pharmacol Toxicol*. 1998;38:97–120.
10. Kamei D, et al. Reduced pain hypersensitivity and inflammation in mice lacking microsomal prostaglandin e synthase-1. *J Biol Chem*. 2004; 279(32):33684–33695.
11. Trebino CE, et al. Impaired inflammatory and pain responses in mice lacking an inducible prostaglandin E synthase. *Proc Natl Acad Sci U S A*. 2003; 100(15):9044–9049.
12. Park JY, Pillinger MH, Abramson SB. Prostaglandin

E2 synthesis and secretion: the role of PGE2 synthases. *Clinical immunology*. 2006;119(3):229–240.
13. Legler DF, Bruckner M, Uetz-von Allmen E, Krause P. Prostaglandin E2 at new glance: novel insights in functional diversity offer therapeutic chances. *Int J Biochem Cell Biol*. 2010;42(2):198–201.
14. Haziot A, et al. Resistance to endotoxin shock and reduced dissemination of gram-negative bacteria in CD14-deficient mice. *Immunity*. 1996;4(4):407–414.
15. Jiang Z, et al. CD14 is required for MyD88-independent LPS signaling. *Nat Immunol*. 2005;6(6):565–570.
16. Iniguez MA, Martinez-Martinez S, Punzon C, Redondo JM, Fresno M. An essential role of the nuclear factor of activated T cells in the regulation of the expression of the cyclooxygenase-2 gene in human T lymphocytes. *J Biol Chem*. 2000; 275(31):23627–23635.
17. Zanoni I, et al. Similarities and differences of innate immune responses elicited by smooth and rough LPS [published online ahead of print December 19, 2011]. *Immunol Lett*. doi:10.1016/j.imlet.2011.12.002.
18. Granucci F, Ferrero E, Foti M, Aggujaro D, Vettoretto K, Ricciardi-Castagnoli P. Early events in dendritic cell maturation induced by LPS. *Microbes Infect*. 1999;1(13):1079–1084.
19. Svensson HG, West MA, Mollahan P, Prescott AR, Zaru R, Watts C. A role for ARF6 in dendritic cell podosome formation and migration. *Eur J Immunol*. 2008;38(3):818–828.
20. De Trez C, Magez S, Akira S, Ryffel B, Carlier Y, Muraille E. iNOS-producing inflammatory dendritic cells constitute the major infected cell type during the chronic Leishmania major infection phase of C57BL/6 resistant mice. *PLoS Pathog*. 2009;5(6):e1000494.
21. Copin R, De Baetselier P, Carlier Y, Letesson JJ, Muraille E. MyD88-dependent activation of B220-CD11b+LY-6C+ dendritic cells during Brucella melitensis infection. *J Immunol*. 2007;178(8):5182–5191.
22. Kissenpfennig A, et al. Dynamics and function of Langerhans cells in vivo: dermal dendritic cells colonize lymph node areas distinct from slower migrating Langerhans cells. *Immunity*. 2005;22(5):643–654.
23. Henri S, et al. Disentangling the complexity of the skin dendritic cell network. *Immunol Cell Biol*. 2010;88(4):366–375.
24. Hochweller K, Striegler J, Hammerling GJ, Garbi N. A novel CD11c.DTR transgenic mouse for depletion of dendritic cells reveals their requirement for homeostatic proliferation of natural killer cells. *Eur J Immunol*. 2008;38(10):2776–2783.
25. Ammirante M, Luo JL, Grivennikov S, Nedospasov S, Karin M. B-cell-derived lymphotoxin promotes castration-resistant prostate cancer. *Nature*. 2010;464(7286):302–305.
26. Itano AA, et al. Distinct dendritic cell populations sequentially present antigen to CD4 T cells and stimulate different aspects of cell-mediated immunity. *Immunity*. 2003;19(1):47–57.
27. Klechevsky E, Kato H, Sponaas AM. Dendritic cells star in Vancouver. *J Exp Med*. 2005;202(1):5–10.
28. Klechevsky E, et al. Functional specializations of human epidermal Langerhans cells and CD14+ dermal dendritic cells. *Immunity*. 2008;29(3):497–510.
29. Harizi H, Gualde N. The impact of eicosanoids on the crosstalk between innate and adaptive immunity: the key roles of dendritic cells. *Tissue Antigens*. 2005;65(6):507–514.
30. Randolph GJ, Sanchez-Schmitz G, Angeli V. Factors and signals that govern the migration of dendritic cells via lymphatics: recent advances. *Springer Semin Immunopathol*. 2005;26(3):273–287.
31. Nagamachi M, et al. Facilitation of Th1–mediated immune response by prostaglandin E receptor EP1. *J Exp Med*. 2007;204(12):2865–2874.
32. Betz M, Fox BS. Prostaglandin E2 inhibits production of Th1 lymphokines but not of Th2 lymphokines. *J Immunol*. 1991;146(1):108–113.
33. Sugimoto Y, Narumiya S. Prostaglandin E receptors. *J Biol Chem*. 2007;282(16):11613–11617.
34. Legler DF, Bruckner M, Uetz-von Allmen E, Krause P. Prostaglandin E2 at new glance: novel insights in functional diversity offer therapeutic chances. *Int J Biochem Cell Biol*. 2010;42(2):198–201.
35. Perera PY, Vogel SN, Detore GR, Haziot A, Goyert SM. CD14-dependent and CD14-independent signaling pathways in murine macrophages from normal and CD14 knockout mice stimulated with lipopolysaccharide or taxol. *J Immunol*. 1997;158(9):4422–4429.
36. Poltorak A, Ricciardi-Castagnoli P, Citterio S, Beutler B. Physical contact between lipopolysaccharide and toll-like receptor 4 revealed by genetic complementation. *Proc Natl Acad Sci U S A*. 2000;97(5):2163–2167.
37. Triantafilou M, Triantafilou K. Lipopolysaccharide recognition: CD14, TLRs and the LPS-activation cluster. *Trends Immunol*. 2002;23(6):301–304.
38. Legler DF, Krause P, Scandella E, Singer E, Groettrup M. Prostaglandin E2 is generally required for human dendritic cell migration and exerts its effect via EP2 and EP4 receptors. *J Immunol*. 2006;176(2):966–973.
39. Kabashima K, Sakata D, Nagamachi M, Miyachi Y, Inaba K, Narumiya S. Prostaglandin E2-EP4 signaling initiates skin immune responses by promoting migration and maturation of Langerhans cells. *Nat Med*. 2003;9(6):744–749.
40. Yen JH, Khayrullina T, Ganea D. PGE2-induced metalloproteinase-9 is essential for dendritic cell migration. *Blood*. 2008;111(1):260–270.
41. Allenspach EJ, Lemos MP, Porrett PM, Turka LA, Laufer TM. Migratory and lymphoid-resident dendritic cells cooperate to efficiently prime naive CD4 T cells. *Immunity*. 2008;29(5):795–806.
42. Cheong C, et al. Microbial stimulation fully differentiates monocytes to DC-SIGN/CD209(+) dendritic cells for immune T cell areas. *Cell*. 2010;143(3):416–429.
43. Cavanagh LL, et al. Activation of bone marrow-resident memory T cells by circulating, antigen-bearing dendritic cells. *Nat Immunol*. 2005; 6(10):1029–1037.
44. Rosenblum MD, Gratz IK, Paw JS, Lee K, Marshak-Rothstein A, Abbas AK. Response to self antigen imprints regulatory memory in tissues. *Nature*. 2011;480(7378):538–542.